ACS APPLIED MATERIALS & INTERFACES

www.acsami.org

Research Article

Highly Reproducible and Sensitive Electrochemiluminescence Biosensors for HPV Detection Based on Bovine Serum Albumin Carrier Platforms and Hyperbranched Rolling Circle Amplification

Yinghao He, Yinhuan Liu, Lingjun Cheng, Yuanyuan Yang, Bin Qiu, Longhua Guo, Yan Wang,* Zhenyu Lin,* and Guolin Hong*

Cite This: *ACS Appl. Mater. Interfaces* 2021, 13, 298−305

Read Online

ACCESS | Metrics & More | Article Recommendations | Supporting Information

ABSTRACT: Most DNA-based electrochemiluminescence (ECL) biosensors are established through the self-assembly of thiolated single-stranded DNA (ssDNA) probes on the Au electrode surface. Because of this random assembly process, a significant discrepancy exists in the distribution of a modified DNA film on different electrodes, which greatly affects the reproducibility of a biosensor. In this study, a porous bovine serum albumin (BSA) layer was first modified on the electrode surface, which can improve the position distribution and spatial orientation of the self-assembly ssDNA probe. It was then coupled with hyperbranched rolling circle amplification to develop the high-reproducibility-and-sensitivity ECL biosensor for human papillomavirus 16 E6 and E7 oncogene detection. In the presence of the target DNA, the surface of the electrode accumulates abundant amplified products through reaction, which contain double-stranded DNA (dsDNA) fragments of different lengths, followed by plentiful dichlorotris (1,10-phenanthroline) ruthenium(II) hydrate ($Ru(phen)_3^{2+}$, acting as an ECL indicator) insertion into grooves of dsDNA fragments, and a strong signal can be detected. There is a linear relationship between the signal and the target concentration range from 10 fM to 15 pM, and the detection limit is 7.6 fM (S/N = 3). After the BSA modification step, the relative standard deviation was reduced from 9.20 to 3.96%, thereby achieving good reproducibility. The proposed ECL strategy provides a new method for constructing high-reproducibility-and-sensitivity ECL biosensors.

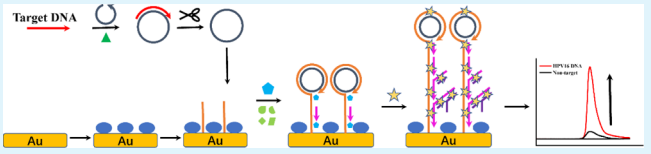

KEYWORDS: *electrochemiluminescence, bovine serum albumin carrier platform, hyperbranched rolling circle amplification, human papillomavirus, high reproducibility*

1. INTRODUCTION

Electrochemiluminescence (also known as electrogenerated chemiluminescence, abbreviated as ECL) has an extremely low background noise, a wide linear range, and high accuracy and sensitivity.[1−4] In practical applications, ECL biosensors have fast response speed, simple operation process, low-cost equipment, and low sample volume.[5] Therefore, they have been widely applied in numerous fields, such as fundamental studies, environmental monitoring, food, and clinical diagnosis.[6,7] Many DNA-based ECL biosensors have been developed to detect DNA,[8] RNA,[9] and proteins[10,11] with high sensitivity. Most of these biosensors require the self-assembly of thiolated single-stranded DNA (ssDNA) probes on the Au electrode surface through Au−S covalent bonds, and then unoccupied sites are blocked with alkanethiol. Unfortunately, it is virtually impossible to precisely control the position and spatial orientation of a probe when it forms a self-assembled monolayer (SAM) on the electrode surface. Therefore, the reproducibility of the detection signal is affected. To overcome this disadvantage, ratiometric ECL sensing technology has been applied in some previous works.[12−14] For instance, Ye et al. developed a dual-wavelength ratiometric ECL immunosensor that successfully detected cardiac troponin I in human serum samples.[15] However, construction of a ratiometric ECL biosensor requires suitable anodic/cathodic emitters and coreactants. Additionally, the electrode surface modification process is complicated and can cause the impedance change to affect the signal. Moreover, under certain circumstances, a special wavelength-resolvable ECL instrument is required.[12] To avoid these tedious requirements, Ni et al. proposed an immobilization-free homogeneous ECL strategy[16] based on the difference in electrostatic repulsion between short and long DNA strands and the surface of indium tin oxide electrodes to improve the reproducibility of detection. Although this strategy has achieved good results, the possible matrix interference limits its widespread use in biological detection. Hence, it is

Received: November 20, 2020
Accepted: December 21, 2020
Published: December 31, 2020

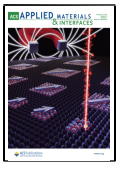

https://dx.doi.org/10.1021/acsami.0c20742
ACS Appl. Mater. Interfaces 2021, 13, 298−305

necessary to develop a simple strategy to improve the reproducibility of ECL biosensors.

Recently, Liu et al. proposed a DNA probe carrier platform based on bovine serum albumin (BSA) to improve the reproducibility of electrochemical biosensors. This platform first assembled BSA on the Au electrode surface to form a porous layer with regular gaps; subsequently, modified probes can be assembled in these pores, resulting in the improvement of the position distribution and spatial orientation of probes, and the interaction between the probe and the target is promoted.[17] As a result, the reproducibility of the biosensor can be greatly improved. With the above advantages, Liu et al. and Chen et al. designed biosensors for detecting cryptococcus neoformans[18] and HBV genotypes[19] and achieved good results. To the best of our knowledge, this technique has not been applied to improve the reproducibility of DNA-based ECL biosensors.

In this study, the BSA carrier platform has been applied to construct a high-reproducibility ECL biosensor for the first time. Human papillomavirus 16 (HPV16) E6 and E7 oncogenes have been chosen as model targets because HPV16 infection is the leading cause of cervical cancer, and E6 and E7 oncogenes play important roles in its pathological process.[20−23] Because of the extremely low concentration of viral DNA in clinical cervical samples,[24] it is necessary to amplify the signal to satisfy the requirement of clinical sample detection. The most widely known strategy is polymerase chain reaction,[25] which requires a distinct thermostable DNA polymerase and a thermal cycler to control temperature cycling, but simple isothermal nucleic acid amplification methods need to be developed to overcome these limitations.[26] Hyperbranched rolling circle amplification (HRCA) is a simple and effective isothermal signal amplification that can perform strand extension and displacement simultaneously, producing a "hyperbranched" DNA complex containing plentiful ssDNA and double-stranded DNA (dsDNA) fragments of different lengths[26,27] and has been applied to develop a variety of sensitive biosensors.[28−30] The porous BSA layer can improve the position distribution and spatial orientation of the capture probe modified on the Au electrode. Therefore, the hybridization between the capture probe and circular padlock probe is promoted, and the subsequent HRCA reaction efficiency is improved because of the improvement of local steric hindrance. Considering the above effects, the biosensor exhibits improved reproducibility and has achieved good results in clinical sample detection. This strategy also provides a new method for the further development of DNA-based ECL biosensors.

2. EXPERIMENTAL SECTION

2.1. Materials. All oligonucleotides used in this study were synthesized and provided by Shanghai Sangon Biotechnology Co., Ltd. (Shanghai, China). These specific sequences are demonstrated as follows:

Target DNA: 5′-ACCGATTTCGGTTACGCCCT-3'

Capture probe: 5′−SH−TTTTTTTTTTGTTCACACA-CACTCTGGATT-3'

Padlock probe: 5′-P-**CGAAATCGGT**AATGGTAGG-TAAGCTGCTAG*AATCCAGAGTGTGTGTGAAC***AGGGCG-TAAC**-3'

Primer 1: 5′-GTTCACACACACTCTGGATT-3'

Primer 2: 5′-AATGGTAGGTAAGCTGCTAG-3'

HPV18 DNA: 5′-GGAATGCTCGAAGGTCGTCT-3'

HPV31 DNA: 5′-GGTGAACCGAAAACGGTTGG-3'

HPV58 DNA: 5′-ACAGCTAGGGCACACAATGG-3'

The sequence marked in bold at the two ends of the padlock probe exactly matches the target DNA, and the sequence marked in italics is complementary to primer 1; moreover, the underlined part is the same as the primer 2 sequence. The portion of the capture probe labeled with the wavy line refers to the same sequence as primer 1.

A deoxynucleotide (dNTP) solution mixture and BSA were also obtained from Shanghai Sangon Biotechnology Co., Ltd. (Shanghai, China). Furthermore, BSA was used directly without any purification. Exonuclease I and Exonuclease III (Exo I and Exo III), as well as the corresponding buffer solutions, were provided by Thermo Fisher Scientific (Shanghai, China). Adenosine 5′-triphosphate (ATP), Bst DNA polymerase (large fragment), T4 DNA ligase, and their corresponding buffer solutions were purchased from New England BioLabs (Beijing, China). Dichlorotris (1,10-phenanthroline) ruthenium(II) hydrate ($Ru(phen)_3^{2+}$) was purchased from Sigma-Aldrich Chemical Co., Ltd. (St. Louis, USA). Tripropylamine (TPA) was obtained from Aladdin (Shanghai, China). Xiamen Biovision Biotechnology Co., Ltd. (Xiamen, China) provided SYBR Green I (10,000×). All other chemicals used throughout the entire experiment were analytical-grade reagents and ultrapure water (resistance of 18.2 MΩ) supplied by the Millipore Direct-Q3 UV system (Bedford, USA). The buffers applied throughout this study were configured as follows. The hybridization buffer solution contained 50 mM NaCl, 10 mM $MgCl_2$, and 10 mM Tris−HCl (pH 7.4). The phosphate buffer solution contained 10 mM Na_2HPO_4, 10 mM NaH_2PO_4, and 0.1 M NaCl (pH 7.4).

2.2. Preparation of the Circular Padlock Probe Solution. The padlock probe (ultimate concentration of 1 μM) was added to a 50 μL volume of hybridization buffer containing different concentrations of target DNA and then incubated at 37 °C for 30 min. Thereafter, to initiate the ligation reaction, a 15 μL solution containing 10 mM ATP, 10 U T4 DNA ligase, and its corresponding buffer was added to the above solution and incubated at 37 °C for 30 min and then at 65 °C for 20 min to deactivate the ligase. Then, Exo I and Exo III were added and incubated at 37 °C for 1 h. Finally, the cells were incubated at 80 °C for 20 min to deactivate the exonucleases. The aforementioned solution was either used immediately or stored at 4 °C.

2.3. Preparation of the ECL Biosensor. To obtain a mirror surface, the gold electrode (2 mm in diameter) was sequentially polished with alumina slurries of 1.0, 0.3, and 0.05 μm, followed by sonication in ethanol and ultrapure water for 3 min, followed by drying with nitrogen.[31] Thereafter, the gold electrode was scanned at a cycling potential of −0.2 to 1.6 V in 0.5 M sulfuric acid solution to obtain a typical stable voltammetric peak. Finally, the electrode was rinsed with ultrapure water and dried under nitrogen for later use. Subsequently, 7 μL of the phosphate buffer containing 5 mg/mL BSA was dropped on the electrode surface and incubated at room temperature for 20 min. Then, 7 μL of a 0.5 μM capture probe solution was dropped on the surface of the BSA-modified gold electrode and incubated at 37 °C for 3 h to modify the electrode through the Au−S covalent bond. Afterward, the modified electrode was soaked in the circular padlock probe solution and kept at 37 °C for 1 h to hybridize the circular padlock probe with the capture probe. Next, the resulting electrode was immersed in a 100 μL solution containing 10 U Bst DNA polymerase and its corresponding buffer solution, 1 μM primer 1, 1 μM primer 2, and 0.8 mM dNTPs to perform the HRCA reaction by incubating at 65 °C for 1 h, and then the Bst DNA polymerase was deactivated by incubating at 80 °C for 20 min. After the amplification reaction, the obtained electrode was immersed in $Ru(phen)_3^{2+}$ solution (1 mM) and incubated for 3 h at 37 °C to intercalate $Ru(phen)_3^{2+}$ molecules into the dsDNA grooves. It is worth noting that the electrode was thoroughly rinsed with ultrapure water and dried under nitrogen after each step.

2.4. ECL Determination. The ECL measurement was carried out with a CHI660D electrochemical system (Shanghai, China) and a BPCL Ultraweak luminescence analyzer (Institute of Biophysics, Chinese Academy of Science, Beijing, China). The achieved electrode, Ag/AgCl electrode, and platinum wire served as the working

https://dx.doi.org/10.1021/acsami.0c20742
ACS Appl. Mater. Interfaces 2021, 13, 298−305

Scheme 1. Mechanism of the Proposed ECL Biosensor for Detecting HPV16 DNA

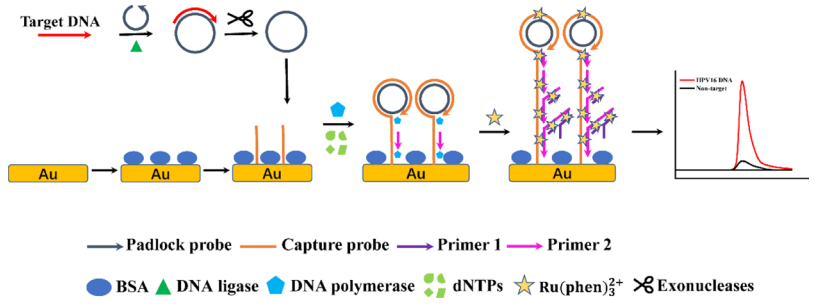

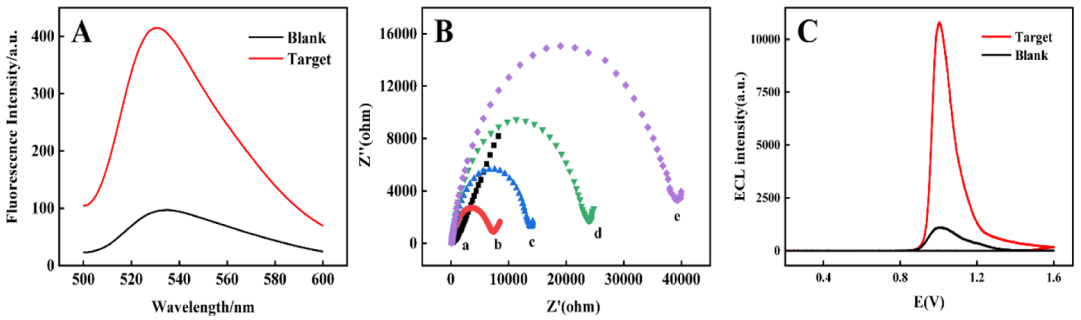

Figure 1. (A) Fluorescence measurement of HRCA amplification products. (B) EIS during different modification and reaction stages: (a) bare Au electrode, (b) bare Au electrode + BSA, (c) electrode b + capture probe, (d) electrode c + circular padlock probe, (e) after HRCA is performed on electrode d; (C) ECL signals of the proposed biosensor in the presence (red line) and absence (black line) of target DNA; the concentration of target DNA was 10 pM.

electrode, reference electrode, and counter electrode, respectively. ECL determination was performed in a phosphate buffer solution containing 20 mM TPA; the signal from the proposed ECL biosensor was measured in the potential range of 0.2−1.6 V, and the scan rate was set at 100 mV/s. Three measurements were taken for each sample, and the average value was used as the reference result. The error bars illustrate the standard deviation of the three repeated measurements. All measurement experiments were performed at room temperature.

2.5. Fluorescence Measurement and Electrochemical Impedance Spectroscopy Determination. To verify whether target DNA can trigger the designed oligonucleotides to initiate the signal amplification of the HRCA reaction, an F-4600 Fluorescence Spectrophotometer (Hitachi High-Technologies Corporation, Tokyo, Japan) was used to perform the fluorescence measurement in this study. The products of the amplification reaction were mixed with SYBR Green I (ultimate concentration of 1×) and then incubated in the dark at room temperature for 15 min. The fluorescence excitation wavelength was 488 nm, and emission spectra were recorded from 500 to 600 nm.

A CHI660A electrochemical system (Shanghai, China) was used to record the electrochemical impedance spectroscopy (EIS) to further verify the reliability of the proposed strategy. The modified electrode, Ag/AgCl electrode, and platinum wire were applied as the working electrode, reference electrode, and counter electrode, respectively. The AC impedance method was performed in a solution containing 10 mM $K_3[Fe(CN)_6]/K_4[Fe(CN)_6]$ (1:1) and 0.1 M KCl to monitor the change in the electron transfer resistance (R_{et}) on the electrode surface after each modification and reaction step.

2.6. Preparation of the Clinical Sample. To verify the feasibility of the proposed ECL biosensor to detect HPV16 DNA in practical applications, cervical brush samples of patients who attended the First Affiliated Hospital of Xiamen University were collected and tested by the proposed strategy, and the results were evaluated. The clinical sample denaturing solution preparation method was the same as in our previous work.[32] To be brief, the denaturation reagent of digene® HC2 high-risk HPV DNA TEST kit was added to each cervical brush sample and incubated at 65 °C for 45 min. Subsequently, the above solution was sonicated in an ice-water bath for 30 min by a Scientz-II D Ultrasonic pulverizer (Zhejiang, China). Finally, the aforementioned solution was heated at 95 °C for 5 min and immediately placed in an ice-water bath. The obtained sample denaturing solution was either detected immediately or stored at 4 °C.

The study was approved by the local ethics committee of the First Affiliated Hospital of Xiamen University and is in line with the Declaration of Helsinki (2008). All written informed consent was obtained for all participants.

3. RESULTS AND DISCUSSION

3.1. Mechanism of the Proposed ECL Biosensor. Scheme 1 demonstrates the mechanism of the proposed ECL strategy. The ellipsoidal BSA molecules self-assemble on the surface of the Au electrode and form a porous layer with regular gaps. The thiolated capture probes are then immobilized in these gaps. Consequently, the assembled probes are evenly distributed on the electrode surface, and the randomness of the probe assembly is reduced. In the presence of target DNA, the terminal regions of the padlock probe can be hybridized with target DNA to bring the 5′ end and 3′ end of the probe close to each other, and then a padlock circular probe is formed under the action of T4 DNA ligase. Afterward, only the circular padlock probe remains in the solution by the shearing of Exos I and III. When the circular padlock probe hybridizes with the capture probe, the HRCA reaction takes place on the electrode surface. Specifically, with the help of Bst DNA polymerase, the capture probe is extended from its 3′ end to generate ssDNA under isothermal conditions, which becomes the template for primer 2 binding. After primer 2 is subsequently hybridized with complementary ssDNA, it is further extended under the action of the DNA polymerase and displaces the downstream growing DNA strands, resulting in the provision of more binding sites for primer 1 to hybridize and extend from its 3′ end. Thereafter,

https://dx.doi.org/10.1021/acsami.0c20742
ACS Appl. Mater. Interfaces 2021, 13, 298−305

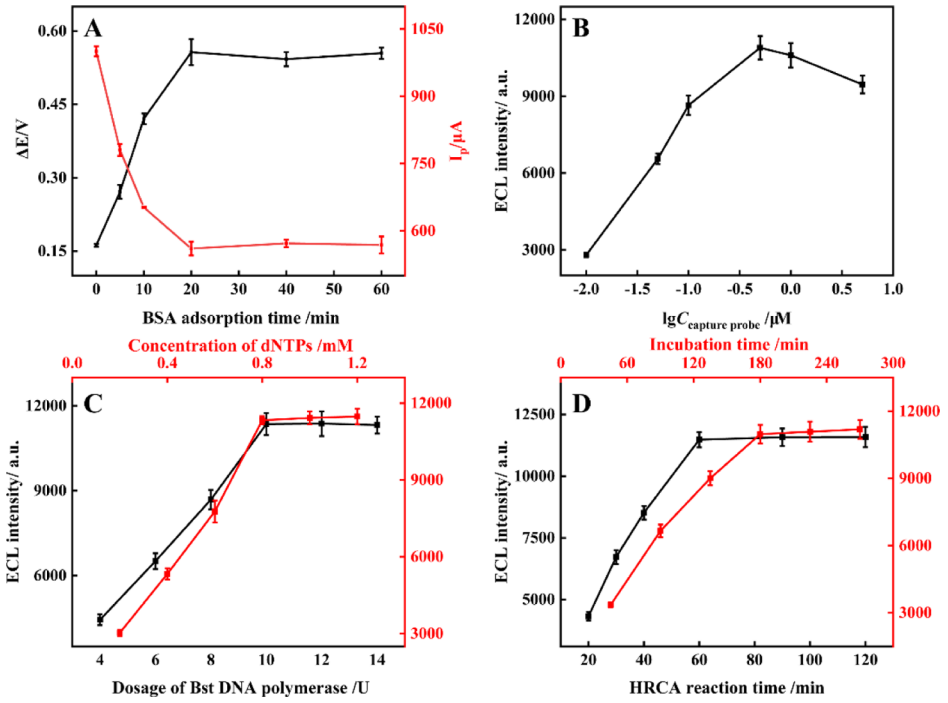

Figure 2. Effects of (A) BSA adsorption time; (B) concentration of the capture probe; (C) dosage of Bst DNA polymerase and the concentration of dNTPs; (D) HRCA reaction time and incubation time of $Ru(phen)_3^{2+}$. The concentration of the capture probe is expressed in a logarithmic form. The concentration of target DNA was 10 pM.

the aforementioned reaction process occurs again. As a result, abundant HRCA products containing dsDNA fragments of different lengths are gathered on the surface of the modified electrode. After the amplification reaction, $Ru(phen)_3^{2+}$, as the ECL indicator, is added to the reaction system, which can be spontaneously inserted into grooves of dsDNA fragments to provide the obvious ECL signal on the electrode surface for detection. Conversely, in the absence of target DNA, the circular padlock probe cannot be generated, and the subsequent HRCA reaction cannot be performed, so only a weak ECL signal generated by the indicator nonspecifically adsorbed on the capture probe can be detected. It is worth noting that the ECL intensity of the proposed biosensor is related to the concentration of target DNA, thereby realizing quantitative determination.

Fluorescence analysis and EIS and ECL determination were applied to verify the feasibility of the proposed strategy. As shown in Figure 1A, in the presence of target DNA (HPV16 DNA), a significant fluorescence signal was observed. In contrast, in the absence of target DNA, only a weak fluorescence signal was detected. The reason for the above phenomenon is that target DNA was able to trigger the designed oligonucleotide to initiate signal amplification of the HRCA reaction to generate plenty of dsDNA fragments, and SYBR Green I can be inserted into dsDNA and enhance the fluorescence intensity.[33] Therefore, it is preliminarily confirmed that the designed sequence is feasible.

Figure 1B demonstrates impedance changes during different modification and reaction steps. Compared with the bare gold electrode (curve a), the impedance of the BSA-modified Au electrode increased significantly (curve b) because BSA was negatively charged at a pH of 7.40, resulting in electrostatic repulsion between $[Fe(CN)_6]^{3-/4-}$ and the BSA layer and preventing $[Fe(CN)_6]^{3-/4-}$ from reaching the surface of the modified electrode for the redox reaction; consequently, the electron transfer rate became slow and increased in impedance. Because the negatively charged DNA phosphate backbone can further prevent $[Fe(CN)_6]^{3-/4-}$ from reaching the electrode surface, after the electrode surface was further modified with the capture probe, a further increase in impedance was observed (curve c). The hybridization between the capture probe and circular padlock probe, the steric hindrance and electrostatic repulsion on the electrode surface continued to increase, and the electrode surface impedance further increased (curve d). After the HRCA reaction was performed on the electrode surface, a vast amount of DNA amplification products accumulated on the electrode surface, and thus the electrode surface impedance further increased (curve e). These phenomena indicate that BSA and the capture probe can be successfully modified sequentially on the surface of the Au electrode, and in the presence of target DNA, the signal can be amplified through HRCA reactions on the electrode surface.

The ECL characteristics of the strategy were further studied to verify the feasibility. In the presence of target DNA, because abundant $Ru(phen)_3^{2+}$ was inserted into amplified dsDNA fragments that accumulated on the electrode surface, a significant ECL signal was detected. Conversely, in the absence of target DNA, the capture probe only nonspecifically adsorbed a very small amount of $Ru(phen)_3^{2+}$, so a weak ECL signal could be detected. Given the above phenomena, the proposed biosensor is feasible for detecting HPV16 DNA.

3.2. Optimization of the Experimental Conditions. To achieve the best detection performance of the ECL biosensor, some reaction conditions have been optimized. Because the modified BSA on the Au electrode surface was very important to the structure of the biosensor, and because it has been confirmed in previous work that BSA requires sufficient time to form a porous layer on the electrode surface,[17] the adsorption time of BSA was first optimized. The adsorption process of protein on the electrode surface can be monitored by cyclic

https://dx.doi.org/10.1021/acsami.0c20742
ACS Appl. Mater. Interfaces 2021, 13, 298−305

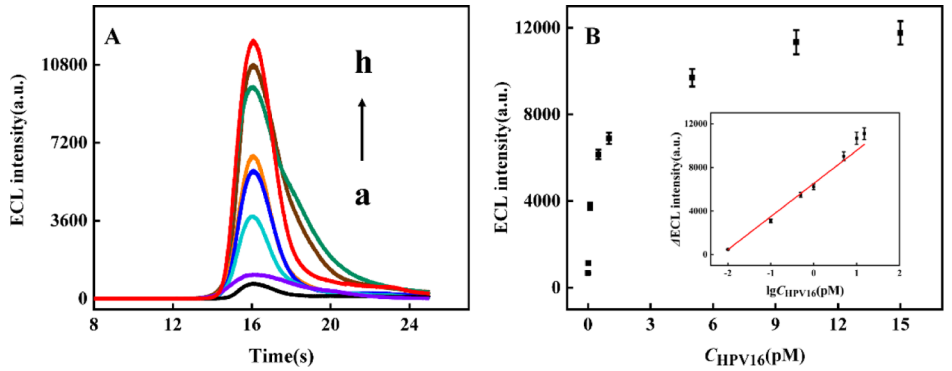

Figure 3. (A) ECL signals of different concentrations of HPV16 DNA. a–h represent the signals at the target DNA concentrations of 0, 10, 100, 500 fM, 1, 5, 10, and 15 pM, respectively. (B) Relationship between HPV16 DNA concentrations and ECL intensities. Insert: calibration curve between the logarithm of HPV16 DNA concentrations and ΔECL.

voltammograms (performed in the solution containing 0.1 M KCl and 10 mM $K_3Fe(CN)_6$, with a potential range from −0.4 to +0.7 V and scan rate of 100 mV/s), in which, as the adsorption time increased, anodic and cathodic peaks broadened, and peak currents decreased simultaneously until the layer was formed. Therefore, in this study, the appropriate adsorption time was determined by observing the change in potential difference between anodic and cathodic peaks (ΔE) and peak currents (I_p). Figure 2A shows that, within 20 min, ΔE increased and I_p decreased gradually, and after 20 min, the changes in ΔE and I_p were slight. This phenomenon indicated that, as the adsorption time increased, BSA was gradually modified on the surface of the Au electrode, which prevented the ferricyanide anion from approaching the electrode surface. Until 20 min, BSA formed a layer on the electrode surface, and thus ΔE and I_p no longer changed. Therefore, the optimized BSA adsorption time was set as 20 min.

The concentration of the capture probe also greatly affects the detection performance of the proposed ECL biosensor. An appropriate concentration can ensure that the prepared electrode can effectively hybridize with a circular padlock probe and avoid excessive local steric hindrance to affect the efficiency of the HRCA reaction, and thus good detection performance can be obtained. As shown in Figure 2B, as the concentration of the capture probe increased, the ECL intensities first increased and then decreased. When the concentration of the capture probe was 0.5 μM, the ECL intensity reached the maximum value. After that, a further increase in the probe concentration led to an increase in the surface steric hindrance of the modified electrode, which affected the amplification efficiency of the HRCA reaction, and therefore, the ECL intensities decreased. To achieve good detection performance, a 0.5 μM capture probe was selected for subsequent experiments.

Because the dosage of Bst DNA polymerase and the concentration of dNTPs are the main factors affecting strand extension and displacement in the HRCA reaction, these factors were subsequently optimized. Figure 2C demonstrates that the ECL intensities increased with increasing dosage of Bst DNA polymerase from 4 to 10 U and then reached a plateau after 10 U, indicating that HRCA amplification products increased with the addition of the DNA polymerase and that 10 U Bst DNA polymerase was sufficient for the HRCA reaction to produce abundant amplification products. Therefore, in this study, 10 U Bst DNA polymerase was applied as the optimized dosage. Subsequently, the concentration of dNTP was optimized because it is another key factor affecting the HRCA reaction. It can be observed that, in the range of 0.2 to 0.8 mM, the ECL intensities increased with increasing dNTP concentration, and beyond 0.8 mM, the ECL signal did not show a further increase; thus, 0.8 mM dNTPs was sufficient for HRCA reactions.

Sufficient HRCA reaction time ensures that a large amount of HRCA products accumulate on the electrode surface. Therefore, optimization of the HRCA reaction time is important to improve the performance of the biosensor. Figure 2D reveals that the ECL intensity of the system first increased significantly with increasing HRCA reaction time and finally reached a plateau after 60 min, indicating that 60 min was sufficient to complete the reaction. In consideration of detection efficiency, 60 min were used in subsequent studies. Moreover, the incubation time for $Ru(phen)_3^{2+}$ insertion into grooves of dsDNA fragments has also been optimized. Within 180 min, the ECL intensity gradually increased and a stable plateau appeared after 180 min, suggesting that 180 min was sufficient for $Ru(phen)_3^{2+}$ to insert into dsDNA to enhance the ECL signal. Therefore, 180 min was chosen as the optimal incubation time of $Ru(phen)_3^{2+}$ for the experiment.

3.3. Performance of the ECL Biosensor. Figure 3A shows the ECL performance of the biosensor with different concentrations of target DNA under the optimal reaction conditions. As the concentrations of HPV16 DNA increased from 0 to 15 pM, the ECL intensities gradually increased. This phenomenon is in accord with the fact that more target DNA can produce more amplification products containing dsDNA fragments with various lengths, which accumulate on the electrode surface, and then more $Ru(phen)_3^{2+}$ can be inserted into dsDNA to amplify the signal. In addition, as shown in Figure 3B, from 10 fM to 15 pM, there is a good linear correlation between the logarithm of target DNA concentration and ΔECL (the ECL intensity changes with and without target), and the regression equation was

$$\Delta ECL = 3036.1 \log C_{HPV16} + 6521.1$$

Here, C_{HPV16} is the concentration of the target DNA (given in units of pM), and the correlation coefficient of R^2 is 0.9927. Moreover, the calculated detection limit is 7.6 fM (S/N = 3). The above results reveal that the ECL biosensor has high sensitivity and an acceptable linear range, demonstrating that it has great potential in practical applications for detecting HPV16 E6 and E7 oncogenes.

https://dx.doi.org/10.1021/acsami.0c20742
ACS Appl. Mater. Interfaces 2021, 13, 298−305

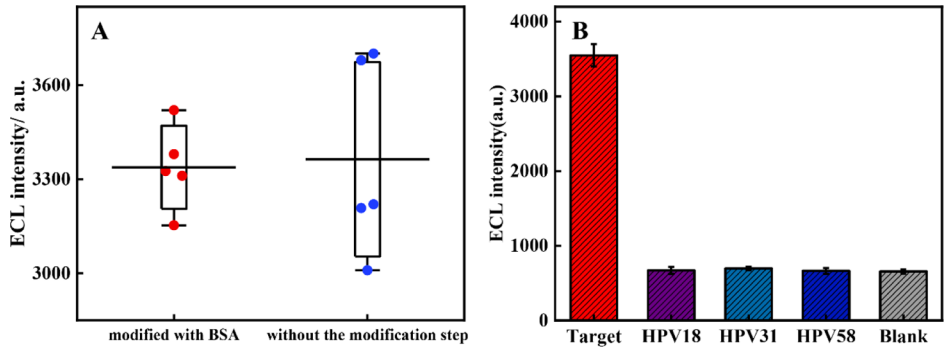

Figure 4. (A) Five consecutive measurements of the ECL signal value of 100 fM target DNA with different electrodes. For the electrode without the modification step, a 7 μL volume of 0.5 μM capture probe solution was dropped directly on the surface, and then unoccupied sites were blocked with alkanethiol. The other operations were the same as for the modified electrode. (B) Selectivity of the proposed ECL biosensor. The concentration of target DNA was 100 fM, and the concentrations of HPV18 DNA, HPV31 DNA, and HPV58 DNA were 10 pM.

The reproducibility of the biosensor was studied by measuring the ECL signals of 100 fM target DNA five consecutive times. As shown in Figure 4A (details in the Supporting Information Table S1), after the BSA modification step, the average value measured by the biosensor changed slightly (from 3364 to 3338), while the relative standard deviation (RSD) decreased from 9.20 to 3.96%. The detection limit and the RSD of the proposed strategy are lower than that of the previously reported HPV biosensors (as shown in Table 1). The reason for the above phenomenon is that, when the electrode is directly modified with a linear single-stranded capture probe, its spatial distribution is quite random, and it can easily lie flat on the electrode surface,[17,34,35] which affects its hybridization with the circular padlock probe and the amplification efficiency. After electrode modification with BSA, the porous layer structure with regular gaps can evenly distribute the capture probe and significantly improve its spatial positioning range and accessibility.[17] Through the modification step, it avoids the high local density of the capture probe to reduce the capture probe/circular padlock probe hybridization efficiency,[36] thereby obtaining a low detection limit and improving the reproducibility of the biosensor.

Table 1. Comparison of Analytical Performance of Different Biosensors for HPV Detection

detection limit	RSD	detection method	Reference
3.8 nM	4.2%	differential pulse voltammetry	[37]
2.3 nM	2.16–7.79%	square-wave voltammetry	[38]
0.03 nM	less than 4.11%	ECL	[39]
1.75 pM	9.3%	differential pulse voltammetry	[40]
0.15 pM	7.1%	electrochemical impedance responses	[41]
7.6 fM	3.96%	ECL	This work

The specificity of the proposed biosensor was evaluated by measuring different DNA sequences, including HPV18, HPV31, HPV58, and HPV16 (the target). It is worth noting that the concentration of HPV18, HPV31, and HPV58 sequences (10 pM) was one hundred times that of the target DNA (100 fM). Figure 4B shows that the ECL signals of the HPV18, HPV31, and HPV58 sequences were not much different from that of the blank control, but the signal caused by adding the target DNA changed greatly. The above results verify the high specificity of the proposed ECL biosensor.

3.4. Application of the Biosensor to Detect Target DNA in Clinical Samples. The proposed biosensor was used to detect HPV16 DNA in clinical samples to further study the applicability of this strategy. Three different levels of DNA sequences (10, 100 fM, and 1 pM) were added to the clinical sample solution by the standard addition method for the recovery study. The experimental results are demonstrated in Table 2. The recoveries range from 96.5 to 105.0%, and the RSDs are between 3.20 and 4.73%. In addition, as shown in Supporting Information Figure S1, the signals of the proposed biosensor have a good linear correlation with the logarithm of the result obtained from the digene® HC2 high-risk HPV DNA TEST kit (the correlation coefficient of R^2 = 0.9790). Such results suggest that the proposed ECL biosensor is competent for clinical analysis.

Table 2. Application of the Biosensor to Detect HPV16 DNA in Clinical Samples

sample	detected (fM)	target DNA added (fM)	total found (fM)	recovery (%)	RSD (%)
no. 1	19.4	10.0	10.3	103.0	3.65
		100.0	101.4	101.4	4.73
		1000.0	964.7	96.5	3.92
no. 2	60.3	10.0	9.7	97.0	3.20
		100.0	104.7	104.7	3.93
		1000.0	965.0	96.5	4.16
no. 3	106.6	10.0	10.5	105.0	3.24
		100.0	101.8	101.8	3.21
		1000.0	1013.9	101.4	3.57

4. CONCLUSIONS

In this study, a simple and effective strategy was developed to improve the reproducibility of ECL biosensors. This method only requires immobilizing BSA on the electrode surface first, improving the position distribution and spatial orientation of the subsequently modified capture probe and promoting the reaction efficiency of HRCA because of the improvement of the local steric effect. Therefore, this simple method can effectively improve the reproducibility of the biosensor. In addition, the biosensor successfully detected HPV16 E6 and E7 oncogenes in clinical samples, demonstrating the good applicability of the proposed strategy. Although the proposed strategy requires a little more time, in practical applications, the amplification reaction can be carried out simultaneously with a

https://dx.doi.org/10.1021/acsami.0c20742
ACS Appl. Mater. Interfaces 2021, 13, 298−305

$Ru(phen)_3^{2+}$ insertion reaction, which can reduce the total time greatly (Supporting Information Figure S2). Considering the above results, the BSA carrier platform can simply and effectively improve the reproducibility of ECL detection strategies and has great potential in clinical trace substance detection, which provides a blueprint for the development of new ECL biosensors.

■ ASSOCIATED CONTENT

Supporting Information

The Supporting Information is available free of charge at https://pubs.acs.org/doi/10.1021/acsami.0c20742.

Comparison of the reproducibility on different electrodes; comparison of the results reached between the proposed method and the reference method; and effects of reaction time on the performance of the proposed sensor (PDF)

■ AUTHOR INFORMATION

Corresponding Authors

Yan Wang − *Department of Cardiology, The Affiliated Cardiovascular Hospital of Xiamen University, Medical College of Xiamen University, Xiamen 361004, People's Republic of China*; Email: 18860089899@139.com

Zhenyu Lin − *Ministry of Education Key Laboratory for Analytical Science of Food Safety and Biology, Fujian Provincial Key Laboratory of Analysis and Detection for Food Safety, Department of Chemistry, Fuzhou University, Fuzhou, Fujian 350116, People's Republic of China*; orcid.org/0000-0001-7890-6812; Email: wyxiamen@126.com

Guolin Hong − *Department of Laboratory Medicine, Xiamen Key Laboratory of Genetic Testing, The First Affiliated Hospital of Xiamen University, Xiamen 361003, People's Republic of China*; Email: zylin@fzu.edu.cn

Authors

Yinghao He − *Department of Laboratory Medicine, Xiamen Key Laboratory of Genetic Testing, The First Affiliated Hospital of Xiamen University, Xiamen 361003, People's Republic of China*

Yinhuan Liu − *Department of Laboratory Medicine, Fuzhou Second Hospital Affiliated to Xiamen University, Fuzhou 350007, People's Republic of China*

Lingjun Cheng − *Department of Laboratory Medicine, Xiamen Key Laboratory of Genetic Testing, The First Affiliated Hospital of Xiamen University, Xiamen 361003, People's Republic of China*

Yuanyuan Yang − *Department of Laboratory Medicine, Xiamen Key Laboratory of Genetic Testing, The First Affiliated Hospital of Xiamen University, Xiamen 361003, People's Republic of China*

Bin Qiu − *Ministry of Education Key Laboratory for Analytical Science of Food Safety and Biology, Fujian Provincial Key Laboratory of Analysis and Detection for Food Safety, Department of Chemistry, Fuzhou University, Fuzhou, Fujian 350116, People's Republic of China*

Longhua Guo − *Ministry of Education Key Laboratory for Analytical Science of Food Safety and Biology, Fujian Provincial Key Laboratory of Analysis and Detection for Food Safety, Department of Chemistry, Fuzhou University, Fuzhou, Fujian 350116, People's Republic of China*

Complete contact information is available at: https://pubs.acs.org/10.1021/acsami.0c20742

Author Contributions

The manuscript was written through contributions of all authors. Y. H., Y. L., and Z. L. conceived the projects. Y. H., Y. L., L. C., Y. Y., and G. H. designed and performed the experiments and collected the data. Y. H., Y. L., L. C., Y. Y., B. Q., L. G., Y. W., Z. L., and G. H. analyzed and discussed the data. All authors discussed the results and contributed to the writing of this manuscript. All authors have given approval to the final version of the manuscript. Y.H. and Y.L contributed equally to this work.

Notes

The authors declare no competing financial interest.

■ ACKNOWLEDGMENTS

This project was financially supported by the National Key Research and Development Program of China (no. 2019YFC1604701), the National Natural Science Foundation of China (81772287, 81371902), and the cooperative project of production and study in the University of Fujian Province (2018Y4007).

■ REFERENCES

(1) Babarniri, B.; Bahari, D.; Salimi, A. Highly sensitive bioaffinity electrochemiluminescence sensors: Recent advances and future directions. *Biosens. Bioelectron.* **2019**, *142*, 111530.

(2) Bertoncello, P.; Forster, R. J. Nanostructured materials for electrochemiluminescence (ECL)-based detection methods: Recent advances and future perspectives. *Biosens. Bioelectron.* **2009**, *24*, 3191−3200.

(3) Delaney, J. L.; Hogan, C. F.; Tian, J.; Shen, W. Electrogenerated Chemiluminescence Detection in Paper-Based Microfluidic Sensors. *Anal. Chem.* **2011**, *83*, 1300−1306.

(4) Li, L.; Liu, H.; Shen, Y.; Zhang, J.; Zhu, J.-J. Electrogenerated Chemiluminescence of Au Nanoclusters for the Detection of Dopamine. *Anal. Chem.* **2011**, *83*, 661−665.

(5) Chen, Y.; Zhou, S.; Li, L.; Zhu, J.-j. Nanomaterials-based sensitive electrochemiluminescence biosensing. *Nano Today* **2017**, *12*, 98−115.

(6) Chinnadayyala, S. R.; Park, J.; Le, H. T. N.; Santhosh, M.; Kadam, A. N.; Cho, S. Recent advances in microfluidic paper-based electrochemiluminescence analytical devices for point-of-care testing applications. *Biosens. Bioelectron.* **2019**, *126*, 68−81.

(7) Khonsari, Y. N.; Sun, S. Recent trends in electrochemiluminescence aptasensors and their applications. *Chem. Commun.* **2017**, *53*, 9042−9054.

(8) Li, M.-X.; Feng, Q.-M.; Zhou, Z.; Zhao, W.; Xu, J.-J.; Chen, H.-Y. Plasmon-Enhanced Electrochemiluminescence for Nucleic Acid Detection Based on Gold Nanodendrites. *Anal. Chem.* **2018**, *90*, 1340−1347.

(9) Zhong, X.; Li, X.; Zhuo, Y.; Chai, Y.; Yuan, R. Synthesizing anode electrochemiluminescent self-catalyzed carbon dots-based nanocomposites and its application in sensitive ECL biosensor for microRNA detection. *Sens. Actuators, B* **2020**, *305*, 127490.

(10) Wang, X.-Y.; Gao, A.; Lu, C.-C.; He, X.-W.; Yin, X.-B.X. B. An electrochemiluminescence aptasensor for thrombin using graphene oxide to immobilize the aptamer and the intercalated Ru(phen)(3)(2+) probe. *Biosens. Bioelectron.* **2013**, *48*, 120−125.

(11) Huang, X.; Zhang, Y.; Xu, W.; Xu, W.; Guo, L.; Qiu, B.; Lin, Z. An ultrasensitive electrochemiluminescence biosensor for nuclear factor kappa B p50 based on the proximity hybridization-induced hybridization chain reaction. *Chem. Commun.* **2019**, *55*, 12980−12983.

(12) Huo, X.-L.; Lu, H.-J.; Xu, J.-J.; Zhou, H.; Chen, H.-Y. Recent advances of ratiometric electrochemiluminescence biosensors. *J. Mater. Chem. B* **2019**, *7*, 6469−6475.
(13) Li, Y.; Wang, L.; Ding, C.; Luo, X. Highly selective ratiometric electrogenerated chemiluminescence assay of DNA methyltransferase activity via polyaniline and anti-fouling peptide modified electrode. *Biosens. Bioelectron.* **2019**, *142*, 111553.
(14) Wang, J.; Song, J.; Zheng, H.; Zheng, X.; Dai, H.; Hong, Z.; Lin, Y. Application of NiFe2O4 nanotubes as catalytically promoted sensing platform for ratiometric electrochemiluminescence analysis of ovarian cancer marker. *Sens. Actuators, B* **2019**, *288*, 80−87.
(15) Ye, J.; Zhu, L.; Yan, M.; Zhu, Q.; Lu, Q.; Huang, J.; Cui, H.; Yang, X. Dual-Wavelength Ratiometric Electrochemiluminescence Immunosensor for Cardiac Troponin I Detection. *Anal. Chem.* **2019**, *91*, 1524−1531.
(16) Ni, J.; Lin, H.; Yang, W.; Liao, Y.; Wang, Q.; Luo, F.; Guo, L.; Qiu, B.; Lin, Z. Homogeneous Electrochemiluminescence Biosensor for the Detection of RNase A Activity and Its Inhibitor. *Anal. Chem.* **2019**, *91*, 14751−14756.
(17) Liu, Y.-H.; Li, H.-N.; Chen, W.; Liu, A.-L.; Lin, X.-H.; Chen, Y.-Z. Bovine Serum Albumin-Based Probe Carrier Platform for Electrochemical DNA Biosensing. *Anal. Chem.* **2013**, *85*, 273−277.
(18) Liu, Y.-H.; Deng, H.-H.; Li, H.-N.; Shi, T.-F.; Peng, H.-P.; Liu, A.-L.; Chen, W.; Hong, G.-L. A DNA electrochemical biosensor based on homogeneous hybridization for the determination of Cryptococcus neoformans. *J. Electroanal. Chem.* **2018**, *827*, 27−33.
(19) Chen, J.; Liu, Z.; Zheng, Y.; Lin, Z.; Sun, Z.; Liu, A.; Chen, W.; Lin, X. B/C genotyping of hepatitis B virus based on dual-probe electrochemical biosensor. *J. Electroanal. Chem.* **2017**, *785*, 75−79.
(20) Bray, F.; Ferlay, J.; Soerjomataram, I.; Siegel, R. L.; Torre, L. A.; Jemal, A. Global cancer statistics 2018: GLOBOCAN estimates of incidence and mortality worldwide for 36 cancers in 185 countries. *Ca-Cancer J. Clin.* **2018**, *68*, 394−424.
(21) Cohen, P. A.; Jhingran, A.; Oaknin, A.; Denny, L. Cervical cancer. *Lancet* **2019**, *393*, 169−182.
(22) Li, K.; Li, Q.; Song, L.; Wang, D.; Yin, R. The distribution and prevalence of human papillomavirus in women in mainland China. *Cancer* **2019**, *125*, 1030−1037.
(23) Jiang, X.; Tang, H.; Chen, T. Epidemiology of gynecologic cancers in China. *J. Gynecol. Oncol.* **2018**, *29*, No. e7.
(24) van Duin, M.; Snijders, P. J. F.; Schrijnemakers, H. F. J.; Voorhorst, F. J.; Rozendaal, L.; Nobbenhuis, M. A. E.; van den Brule, A. J. C.; Verheijen, R. H. M.; Helmerhorst, T. J.; Meijer, C. J. L. M. Human papillomavirus 16 load in normal and abnormal cervical scrapes: An indicator of CINII/III and viral clearance. *Int. J. Cancer* **2002**, *98*, 590−595.
(25) Asiello, P. J.; Baeumner, A. J. Miniaturized isothermal nucleic acid amplification, a review. *Lab Chip* **2011**, *11*, 1420−1430.
(26) Mohsen, M. G.; Kool, E. T. The Discovery of Rolling Circle Amplification and Rolling Circle Transcription. *Acc. Chem. Res.* **2016**, *49*, 2540−2550.
(27) Thomas, D. C.; Nardone, G. A.; Randall, S. K. Amplification of padlock probes for DNA diagnostics by cascade rolling circle amplification or the polymerase chain reaction. *Arch. Pathol. Lab. Med.* **1999**, *123*, 1170−1176.
(28) Cheng, Y.; Zhang, X.; Li, Z.; Jiao, X.; Wang, Y.; Zhang, Y. Highly Sensitive Determination of microRNA Using Target-Primed and Branched Rolling-Circle Amplification. *Angew. Chem., Int. Ed.* **2009**, *48*, 3268−3272.
(29) Wang, Q.; Zheng, H.; Gao, X.; Lin, Z.; Chen, G. A label-free ultrasensitive electrochemical aptameric recognition system for protein assay based on hyperbranched rolling circle amplification. *Chem. Commun.* **2013**, *49*, 11418−11420.
(30) Li, X.-H.; Zhang, X.-L.; Wu, J.; Lin, N.; Sun, W.-M.; Chen, M.; Ou, Q.-S.; Lin, Z.-Y. Hyperbranched rolling circle amplification (HRCA)-based fluorescence biosensor for ultrasensitive and specific detection of single-nucleotide polymorphism genotyping associated with the therapy of chronic hepatitis B virus infection. *Talanta* **2019**, *191*, 277−282.
(31) Yang, L.; Zhang, Y.; Li, R.; Lin, C.; Guo, L.; Qiu, B.; Lin, Z.; Chen, G. Electrochemiluminescence biosensor for ultrasensitive determination of ochratoxin A in corn samples based on aptamer and hyperbranched rolling circle amplification. *Biosens. Bioelectron.* **2015**, *70*, 268−274.
(32) He, Y.; Cheng, L.; Yang, Y.; Chen, P.; Qiu, B.; Guo, L.; Wang, Y.; Lin, Z.; Hong, G. Label-free homogeneous electrochemical biosensor for HPV DNA based on entropy-driven target recycling and hyperbranched rolling circle amplification. *Sens. Actuators, B* **2020**, *320*, 128407.
(33) Bünzli, J. C. G. Lanthanide Luminescence for Biomedical Analyses and Imaging. *Chem. Rev.* **2010**, *110*, 2729−2755.
(34) Li, Z.; Zhao, B.; Wang, D.; Wen, Y.; Liu, G.; Dong, H.; Song, S.; Fan, C. DNA Nanostructure-Based Universal Microarray Platform for High-Efficiency Multiplex Bioanalysis in Biofluids. *ACS Appl. Mater. Interfaces* **2014**, *6*, 17944−17953.
(35) Lin, Y.; Jia, J.; Yang, R.; Chen, D.; Wang, J.; Luo, F.; Guo, L.; Qiu, B.; Lin, Z. Ratiometric Immunosensor for GP73 Detection Based on the Ratios of Electrochemiluminescence and Electrochemical Signal Using DNA Tetrahedral Nanostructure as the Carrier of Stable Reference Signal. *Anal. Chem.* **2019**, *91*, 3717−3724.
(36) Peterson, A. W.; Heaton, R. J.; Georgiadis, R. M. The effect of surface probe density on DNA hybridization. *Nucleic Acids Res.* **2001**, *29*, 5163−5168.
(37) Nasirizadeh, N.; Zare, H. R.; Pournaghi-Azar, M. H.; Hejazi, M. S. Introduction of hematoxylin as an electroactive label for DNA biosensors and its employment in detection of target DNA sequence and single-base mismatch in human papilloma virus corresponding to oligonucleotide. *Biosens. Bioelectron.* **2011**, *26*, 2638−2644.
(38) Teengam, P.; Siangproh, W.; Tuantranont, A.; Henry, C. S.; Vilaivan, T.; Chailapakul, O. Electrochemical paper-based peptide nucleic acid biosensor for detecting human papillomavirus. *Anal. Chim. Acta* **2017**, *952*, 32−40.
(39) Nie, Y.; Zhang, X.; Zhang, Q.; Liang, Z.; Ma, Q.; Su, X. A novel high efficient electrochemiluminescence sensor based on reductive Cu(I) particles catalyzed Zn-doped MoS2 QDs for HPV 16 DNA determination. *Biosens. Bioelectron.* **2020**, *160*, 112217.
(40) Chekin, F.; Bagga, K.; Subramanian, P.; Jijie, R.; Singh, S. K.; Kurungot, S.; Boukherroub, R.; Szunerits, S. Nucleic aptamer modified porous reduced graphene oxide/MoS2 based electrodes for viral detection: Application to human papillomavirus (HPV). *Sens. Actuators, B* **2018**, *262*, 991−1000.
(41) Karimizefreh, A.; Mahyari, F. A.; VaezJalali, M.; Mohammadpour, R.; Sasanpour, P. Impedimetic biosensor for the DNA of the human papilloma virus based on the use of gold nanosheets. *Microchim. Acta* **2017**, *184*, 1729−1737.

https://dx.doi.org/10.1021/acsami.0c20742
ACS Appl. Mater. Interfaces 2021, 13, 298−305